Tetrahedron 66 (2010) 3855–3860

Contents lists available at ScienceDirect

Tetrahedron

journal homepage: www.elsevier.com/locate/tet

Mechanistic elucidation of ketenimine–butynoate cycloaddition reaction: role of biradical intermediates in isotopomeric purity of benzyl (1,1a,6,6a-$^{13}C_4$)-6-methyl anthranilic ester

Armando Navarro-Vázquez [a,b,*], José-Lorenzo Alonso-Gómez [a,b], Johan Lugtenburg [a,b], María-Magdalena Cid [a,b,*]

[a] Departamento de Química Orgánica, Facultade de Química, Universidade de Vigo, Campus Lagoas-Marcosende, 36310 Vigo, Spain
[b] Leiden Institute of Chemistry, Gorlaeus Laboratory, Leiden University, P O Box 9502, 2300 RA Leiden, The Netherlands

ARTICLE INFO

Article history:
Received 5 January 2010
Received in revised form 12 February 2010
Accepted 10 March 2010
Available online 15 March 2010

Keywords:
Ketenimines
Diels–Alder
Biradicals
DFT
Isotopic labeling

ABSTRACT

Thermal Diels–Alder reaction of vinyl ketenimines with ^{13}C-labeled 2-butynoate, efficiently prepared from $^{13}C_4$-acetoacetate via the enol triflate, rendered at 160 °C the corresponding methylanthranilic ester isotopomerically pure. However, when the reaction was run at 100 °C, 7% of isotope exchange between C^{6a} and C^5 was observed. This result is explained through a base-like catalyzed isomerization of the alkyne to the corresponding allene. Combined DFT and coupled-cluster computations show the feasibility of this mechanistic proposal. Better agreement between DFT and coupled-cluster activation and reaction energies is observed for the meta-GGA MPWB1K functional as compared to previous B3LYP results.

© 2010 Elsevier Ltd. All rights reserved.

1. Introduction

The study and analysis of all metabolites in an organism (metabolome) have recently drawn great attention due to their utility in the study of genes functions.[1] Anthranilic acid (**1a**), first dubbed as vitamin L_1, is a metabolite found in the biosynthetic pathway of tryptophan in plants, yeast, and bacteria. The enzyme anthranilate synthase catalyzes the conversion of chorismate into anthranilate in the first reaction leading from the common aromatic amino acid pathway toward the biosynthesis of tryptophan and is subjected to feedback inhibition.[2] However, little is known about the mechanisms that couple regulation of secondary metabolic pathways to the synthesis of primary metabolic precursors.[3] In fact, labeled anthranilic acids were already used to clarify the biosynthetic origin of sweet odorous 2-aminobenzaldehyde in *Hebeloma sacchariolens*.[4]

Moreover, several anthranilate derivatives, including the food flavor 6-methylanthranilate (**1b**), have shown interesting biological activities, i.e., anti-inflammatory,[5] anti-proliferative,[6] and herbicidal,[7] although the mode of action is not fully understood. Consequently, the conjunction of labeled metabolites and NMR and MS techniques would be a useful tool to provide a macroscopic view of the metabolome,[8] and to elucidate the mechanisms of action of such compounds.

As a part of our work in the preparation of ^{13}C-labeled vitamins, we envisioned that $^{13}C_4$-6-methylantranilic ester **2** could be a suitable precursor to prepare the aromatic core of tetralabeled α-tocopherol, the most important fat-soluble antioxidant in tissues and also an essential nutritional supplement (Fig. 1).[9]

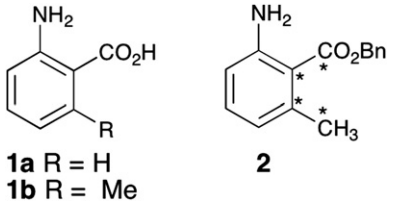

Figure 1. Anthranilic acid derivatives.

We have reported the preparation of benzyl (1,1a,6,6a-$^{13}C_4$)-6-methylanthranilate (**2**) through a Diels–Alder reaction between vinyl ketenimine **3** and benzyl 2,3-butadienoate. Interestingly, we observed by ^1H and ^{13}C NMR spectroscopy that the product of the reaction suffered partial ^{13}C isotope exchange between position 5

* Corresponding authors. Tel.: +34 986813563; fax: +34 986812262; e-mail addresses: armando.navarro@uvigo.es (A. Navarro-Vázquez), mcid@uvigo.es (M.-M. Cid).

0040-4020/$ – see front matter © 2010 Elsevier Ltd. All rights reserved.
doi:10.1016/j.tet.2010.03.035

and the methyl group at position 6.[10] The scrambling of ^{13}C-label was evident by carrying out the reactions with isotopically labeled reagents. This exchange was explained through the reversible formation of a cyclobutane intermediate that strongly supported a stepwise cyclization mechanism. Generally, it is difficult to prove the existence of a stepwise pathway in Diels–Alder reactions, particularly when biradical intermediates are involved, since evidence for such biradical mechanism arises mainly from the loss of stereochemical integrity. However, complete stereospecificity does not necessary mean a concerted mechanism as stereochemistry retention can arise from a very fast coupling of biradical intermediates. Most of the information on these biradical pathways comes from ab initio computations, which in general agree that the archetypal butadiene/ethylene Diels–Alder reaction takes place through a concerted transition state of synchronous nature, whereas a stepwise biradical mechanism lies between 2.3 and 7.7 kcal/mol over the transition state (TS) for a concerted reaction.[11] Note, however, that this difference is not so high and appropriate structural modifications could make both mechanisms competitive.

In our previous synthesis we observed a 91:9 ratio between both anthranilate isotopomers, a fact that can hamper further metabolic routes investigations. In this way, we present here a novel synthesis based on a ketenimine–alkyne Diels–Alder cycloaddition to prepare isotopomerically purer (1,1a,6,6a)-$^{13}C_4$-6-methylanthranilate **2**, along with a computational study of ketenimine–alkyne and ketenimine–allene cycloadditions by means of combined DFT and coupled-cluster computations.

2. Results and discussion

The here presented synthesis of anthranilate **2** involved a Diels–Alder reaction between ketenimine **3** and benzyl (1,2,3,4-$^{13}C_4$)-butynoate (**4**) (Scheme 1). Although **2** with three labeled positions would be sufficient for most of the biochemical studies, we decided to prepare the tetralabeled analogue because ethyl (1,2,3,4-$^{13}C_4$)-acetoacetate is commercially available at reasonable prices and could work as a precursor to compound **4**.

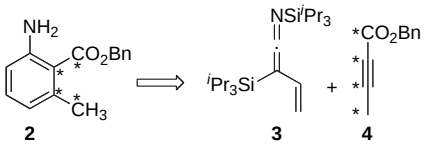

Scheme 1. Retrosynthetic analysis of methylanthranilate **2**.

Ethyl (1,2,3,4-$^{13}C_4$)-acetoacetate was first converted into the corresponding benzyl ester **5** through a transesterification with benzyl alcohol[12] in order to make it more manageable (Scheme 2). The conversion of the acetoacetate into the corresponding inner alkyne **4** turned out to be a difficult task and deprotonation at the less hindered allylic position gave rise to the allene instead. Inspired by a method described for the decarboxylative elimination of enoltriflates,[13] we successfully prepared the desired alkyne through base elimination of the corresponding enoltriflate **6**. Thus, treatment of **5** with NaH in Et_2O followed by addition of triflic anhydride and subsequent elimination of trifluoromethanesulfate with Et_3N in THF at 80 °C, gave benzyl (1,2,3,4-$^{13}C_4$)-but-2-ynoate (**4**) in high yield with total incorporation of ^{13}C-label at each position. Ketenimine **3** was efficiently prepared from crotononitrile by reaction with LDA and triisopropylsilyl chloride following a previously described procedure.[14]

Then, Diels–Alder reaction of alkyne **4** with bis(triisopropyl)-ketenimine **3** rendered intermediates **7a**/**7b**, that after tautomerization and silyl groups deprotection rendered ^{13}C-methylanthranilate **2**/**2b** in 52–69% yield. Surprisingly, as in the case of the Diels–Alder

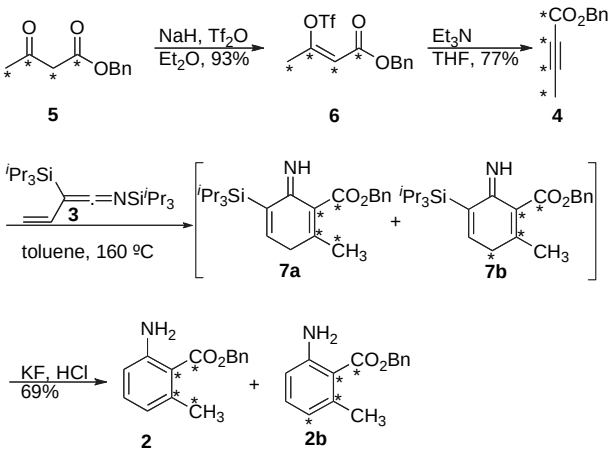

[a] NaH, Tf_2O, Et_2O, 93%; [b] Et_3N, THF, 77%; [c] toluene, 160 ºC; KF, HCl, 69%.

Scheme 2. Synthesis of benzylanthranilate **2**.

reaction of benzyl 2,3-butadienoate, allene **8**,[10] product **2b** was still observed in the reaction of alkyne **4**. As it is shown in Table 1, the ratio between **2**/**2b** was dependent on the temperature and on the ketenimine **3**/alkyne **4** ratio.

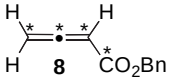

Table 1
Reaction conditions for **3**+**4**→**2**+**2b**

Entry	**3** (mol %)	*T* (°C)	**2**/**2b**[a]	Yield[b] (%)
1	110	100	93:7	45
2	70	140	97:3	25[c]
3	140	140	93:7	51
4	120	160	93:7	27[d]
5	150	160	99:1	40[c]
6	160	160	99:1	52
7	200	160	99:1	69

[a] Ratio measured by ^{1}H NMR integration.
[b] Isolated yields.
[c] Alkyne **4** was recovered.
[d] Allene **8** was recovered.

The data summarized in Table 1 show that when the Diels–Alder reaction between ketenimine **3** and alkyne **4** was run at 100 °C 7% of isotope labeling exchange was observed. The highest isotopomer ratio **2**/**2b** (99:1) was obtained at 160 °C and at least 150% excess of ketenimine **3** was necessary due to its inherent thermal instability. Higher excesses of **3** led to higher reaction yields.

As we have already reported, a reversible [2+2] cycloaddition between allene **8** and ketenimine **3** is responsible for the observed labeling exchange and, as this is not possible for the alkyne, the now observed exchange strongly indicates a previous alkyne–allene isomerization. A solution containing only alkyne **4** was heated at 160 °C over 48 h. ^{1}H NMR monitoring did not show any evidence of isomerization to allene. This suggests the presence of a base-catalyzed alkyne–allene isomerization process or intramolecular rearrangements of reaction intermediates. In addition, the labeling exchange decreases with higher reaction temperature and ketenimine excess. This fact suggests that isomerization is a slow process as compared to cycloaddition and if enough ketenimine is present in the reaction mixture the alkyne cleanly undergoes the [4+2] process.

In order to gain more insight into this type of processes, we have examined both concerted and stepwise reaction pathways for the cycloaddition reaction between butynal, **4c**,[15] and vinyl ketenimine, **3c** (Scheme 3a). Our previous B3LYP studies[10] showed that in the

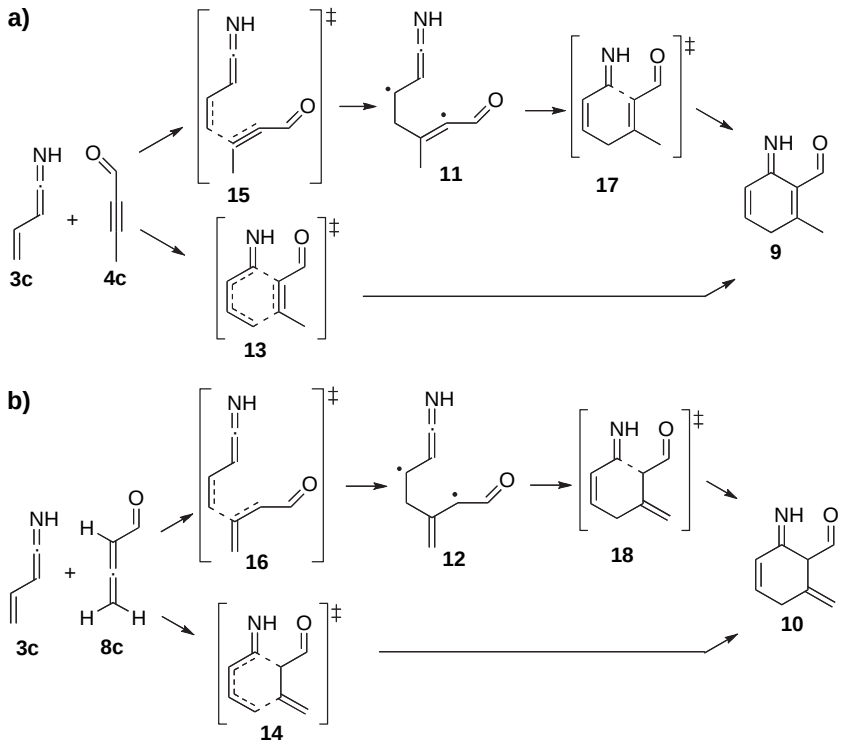

Scheme 3. Comparison of mechanisms for cycloaddition reactions of alkyne **4** (a) and allene **8** (b).

cycloaddition reaction between ketenimine **3c**[15] and allene **8c**[15] a biradical pathway, initiated by the formation of the bond between allene-C^3 and ketenimine-C^4, is energetically feasible. In fact, MPWB1K computations place the transition state for the biradical formation, **16**, 2.1 kcal/mol over the transition state for the concerted process, **14**, lending support to the existence of the stepwise pathway (Scheme 3b).

As it is shown in Figure 2, the alkyne cycloaddition reaction shows a higher barrier for the concerted pathway compared to the allene cycloaddition (43.5 vs 37.8 kcal/mol, MPWB1K). Computations indicate that the stepwise and concerted pathways are energetically closer for the alkyne (43.5 vs 44.0 kcal/mol at MPWB1K), than for the allene case, even though intermediate biradical **11** is much higher in energy than the corresponding allyl biradical **12** (Fig. 2). Note that both biradicals, **11** and **12**, are more stabilized in the DFT UBS computations than in the single point BD(T) results. According to the less stable character of biradical intermediate **11** as compared to **12**, the MPWB1K geometry for the concerted transition structure **13** shows that the reaction of alkyne **4c** is more synchronous than that of allene **8c**, with C^5–C^6 and C^1–C^2 forming bond distances of 2.084 and 2.379 Å vs 1.981 and 2.907 Å in **14**, respectively.

It is worth to note the good agreement between the MPWB1K DFT and the coupled-cluster computations for both activation and, particularly, reaction energies, although caveat should be taken in computation of energies of intermediates with very strong biradical character. This fact promotes the meta-GGA hybrid MPWB1K, in conjunction with an UBS scheme, as a better choice than standard B3LYP functional for studies on cycloaddition reactions involving not only closed-shell concerted transition states but also open-shell singlet biradical intermediates and biradicaloid transition states (see Scheme 3 and Table 2). Further computational studies should

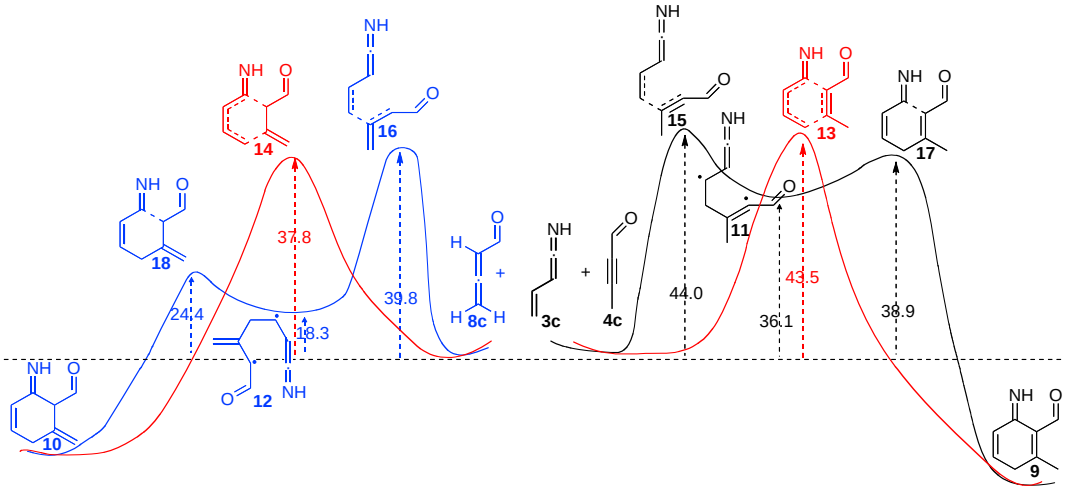

Figure 2. Comparative energy profile for the cycloaddition reaction of **3c** with **4c** or **8c**.

Table 2
Free energies, $\Delta G_{423.15\ K}$ (kcal/mol), for computed species

Species	**13**	**15**	**11**	**17**	**9**
$\Delta G^{a,c}$	43.5	44.0	36.1	38.9	−51.6
$\Delta G^{a,d}$	41.2	42.6	44.2	42.9	−53.3

Species	**14**	**16**	**12**	**18**	**10**	**19**	**20**	**21**
$\Delta G^{b,c}$	37.8	39.8	18.3	24.4	−38.0	−14.9	28.1	27.3
$\Delta G^{b,e}$	38.9	37.9	22.1	29.3	−25.4	−3.7	31.5	30.6
$\Delta G^{b,d}$	36.5	38.7	25.8	25.4	−42.4	−12.8	27.2	26.7

[a] Relative to **3c**+**4c**.
[b] Relative to **3c**+**8c**.
[c] MPWB1K/6-311+G**.
[d] BD(T)/cc-pVDZ//MPWB1K/6-311+G**.
[e] B3LYP/6-31+G* with MPWB1K/6-311+G** thermochemical contributions.

help to better evaluate the performance of meta-GGA functionals for this kind of cycloadditions.

BD(T)//MPWB1K computations have been also performed for the alternative [2+2] cycloaddition reaction, responsible for isotope exchange, between allene **8c** and ketenimine **3c**. Computations put the transition state **20** for [2+2] biradical collapse higher in energy than the alternative [4+2] TS **18** being the BD(T) predicted gap (1.8 kcal/mol) small enough to be compatible with the experimental observation of label scrambling (Scheme 4).

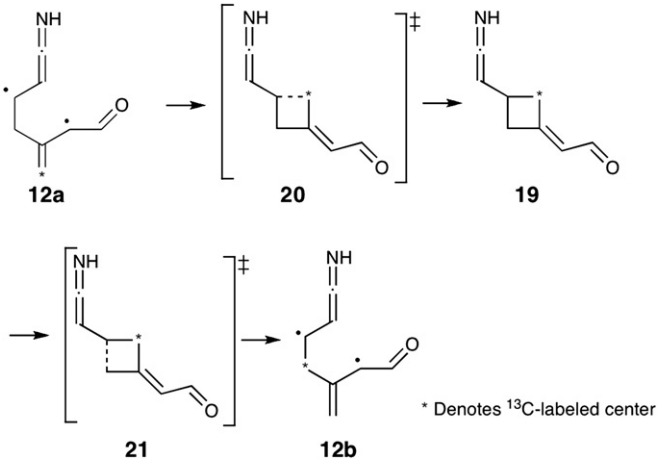

Scheme 4. Stepwise [2+2] cycloaddition.

It should be noted the much better agreement of MPWB1K computed energies for cyclization products **10** and **19** with the BD(T) results as compared to the B3LYP computations, see Table 2, which severely underestimated the exothermicity of the processes, due to the deficient treatment of medium range correlation by this functional.[16]

Although computations placed biradical **11** quite high in energy, we still considered the possibility that the unexpected alkyne–allene isomerization could be caused by a series of rearrangements between biradical intermediates present during a stepwise [4+2] process. A possible mechanistic pathway is the conversion of the biradical **11** into the vinyl–allyl radical **22** through a [1,4]-hydrogen shift. Subsequent [1,4]-H shift on this intermediate gives bisallyl biradical **12**, which dissociates to the corresponding allene **8** and the starting ketenimine **3** (Scheme 5). A further Diels–Alder reaction between allene **8** and ketenimine **3** would account for the label-exchange, as we have already demonstrated.[10]

However, the MPWB1K computed reaction barrier ($\Delta G_{423.15\ K}$), for the conversion of biradical **11** into **22** through [1,4]-H shift is as high as 32.1 kcal/mol, clearly ruling out this possibility, as **11** has to surmount a very low barrier (2.8 kcal/mol at MPWB1K) to collapse to adduct **9**. Consequently, alkyne isomerization is very probably

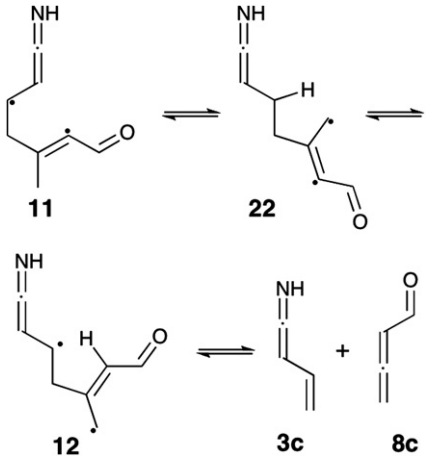

Scheme 5. Plausible mechanism for the formation of allene **8** from alkyne **4** (via biradical **11**).

a base-catalyzed process, either caused by ketenimine itself or by traces of amine-like side products generated in the reaction medium.

3. Conclusions

We have developed an efficient synthetic procedure for fully labeled butynoate **4** from commercially available ethyl $^{13}C_4$-acetoacetate without any labeling loss or any isotope scrambling. Diels–Alder reaction of alkyne **4** and vinyl ketenimine **3** furnished isotopomerically pure methylanthranilate **2**. Temperatures higher than 150 °C are needed in order to avoid labeling scrambling. As an explanation for this observed behavior, we propose a base-catalyzed isomerization of the butynoate **4** to the more stable allene **8**, which is the ultimate responsible for the label-exchange. When single point BD(T) computations were taken as reference, the computational studies showed that DFT modeling of these reactions using a hybrid meta-GGA functional MPWB1K provides a more consistent description as compared to B3LYP. This study shows the value of ^{13}C-labeled compounds combined with computational methods in revealing hidden mechanistic details.

4. Experimental section

4.1. General

Reagents and solvents were purchased as reagent-grade and used without further purification unless otherwise stated. Solvents were dried according to published methods and distilled before use. All reactions were performed in oven-dried or flame-dried glassware under an inert atmosphere of Ar unless otherwise stated. NMR spectra were recorded in a Bruker AMX400 (400.13 MHz and 100.61 MHz for proton and carbon, respectively) spectrometer at 298 K with residual solvent peaks as internal reference and the chemical shifts are reported in δ [ppm], coupling constants J are given in Hz and the multiplicities expressed as follows: s=singlet, d=doublet, t=triplet, q=quartet, m=multiplet. Electronic impact ionization (EI) mass spectra were recorded on a VG-Autospec M instrument.

4.2. Benzyl (1,2,3,4-$^{13}C_4$)-3-trifluoromethanesulfonyloxybut-2-enoate (6)

Benzyl (1,2,3,4-$^{13}C_4$)-acetoacetate (**5**)[10] (196 mg, 1 mmol) in dry Et_2O (7 mL) was added to a prewashed suspension of NaH (60%) (82 mg, 2.04 mmol) in Et_2O (4 mL) at 0 °C and stirred for 1.5 h.

Triflic anhydride (1.05 g, 3.67 mmol) was then added and the reaction mixture was stirred for 1 h more. The mixture was allowed to warm to 25 °C and stirred for 1 h. Satd aq ammonium chloride solution was added followed by extraction with CH_2Cl_2. The organic fractions were washed with 1 M hydrochloric acid solution and brine, dried (Na_4SO_4), and concentrated under reduced pressure. The residue was purified by column chromatography (SiO_2, Hexane/EtOAc, 83:17) to render the enoltriflate **6** (302 mg, 93%). ν_{max} (film)/cm^{-1} 1684; δ_H (400 MHz, $CDCl_3$, TMS) 2.16 (ddd, J=4.8, 6.9, 130.6 Hz, 3H), 5.22 (d, J=3.3 Hz, 2H), 5.80 (ddd, J=2.5, 7.9, 164.8 Hz, 1H), 7.37 (s, 5H) ppm; δ_C (101 MHz, $CDCl_3$, TMS) 20.90 (ddd, J=5.2, 5.8, 51.2 Hz, CH_3, C^4), 66.75 (s, CH_2), 112.3 (ddd, J=5.8, 78.1, 85.1 Hz, CH, C^2), 118.3 (q, J=319.7 Hz, CF_3), 128.4 (s, 2×CH), 128.6 (s, CH), 135.2 (d, J=1.5 Hz, C), 155.7 (ddd, J=1.5, 51.2, 85.1 Hz, C^3), 162.0 (ddd, J=1.5, 5.2, 78.1 Hz, C^1) ppm; δ_F (376 MHz, $CDCl_3$, TMS) −74.6 ppm; HRMS (FAB) m/z 329.0482 ($C_8{}^{13}C_4H_{12}F_3O_5S$ requires 329.0492).

4.3. Benzyl (1,2,3,4-$^{13}C_4$)-but-2-ynoate (4)

A solution of the triflate **6** (820 mg, 2.4 mmol) in Et_2O (70 mL) and Et_3N (4.2 mL, 30 mmol) was stirred at 80 °C for 24 h. The solvent was evaporated and the residue was purified (SiO_2, hexane/EtOAc, 84:16) to give the pure but-2-ynoate **4** (330 mg, 77% yield). ν_{max} (film)/cm^{-1} 2157, 1664; δ_H (400 MHz, $CDCl_3$, TMS) 2.03 (dddd, J=1.8, 4.6, 10.7, 132.8 Hz, 3H), 5.18 (d, J=3.4 Hz, 2H), 7.38–7.33 (m, 5H); δ_C (101 MHz, $CDCl_3$, TMS) 3.7 (ddd, J=1.8, 11.2, 65.9 Hz, CH_3), 67.3 (t, J=1.8 Hz, CH_2), 72.1 (ddd, J=11.2, 127.7, 182.7 Hz, C), 86.0 (ddd, J=20.8, 65.9, 182.7 Hz, C), 128.39 (CH), 128.42 (CH), 128.5 (CH), 135.1 (s, C), 153.4 (ddd, J=1.8, 20.8, 127.7 Hz, C); HRMS m/z 179.0886 ($C_7{}^{13}C_4H_{11}O_2$ requires 179.0893).

4.4. Benzyl (1,1a,6,6a-$^{13}C_4$)-2-amino-6-methyl-benzoate (2)

In a Schlenk tube ketenimine **3** (170 mg, 0.82 mmol) was diluted in toluene (0.2 mL) under argon atmosphere. To this solution, butynoate **4** (45 mg, 0.25 mmol) was added and the mixture was heated at 160 °C for 24 h. After removal of the toluene under reduced pressure, the residue was taken up in MeOH (5.0 mL). Next, KF (160 mg, 2.76 mmol) and a solution of concentrated HCl (0.3 mL, 3.6 mmol) were added and the mixture was refluxed for 2 h. Then, water was added and the solution was neutralized with satd aq $NaHCO_3$ solution. The water layer was extracted with Et_2O; the combined organic layers were washed with brine, dried (Na_2SO_4), and the solvent removed in under reduced pressure. The residue was purified by column chromatography (SiO_2, 100% CH_2Cl_2) affording **2** as a light yellow oil (42 mg, 69%). ν_{max} (film)/cm^{-1} 1646; δ_H (400 MHz, $CDCl_3$, TMS) 2.43 (ddd, J=4.0, 5.9, 128.0 Hz, CH_3), 5.13 (br s, 2H, NH_2), 5.37 (d, J=3.1 Hz, 2H, CH_2), 6.53 (m, 2H, H^3+H^5), 7.08 (m, 1H, H^4), 7.33–7.47 (m, 5H); δ_C (101 MHz, $CDCl_3$, TMS) 23.2 (ddd, J=1.0, 2.1, 43.5 Hz, CH_3, C^{6a}), 66.5 (CH_2), 113.8 (ddd, J=1.7, 61.9, 74.5 Hz, C^1), 114.6 (m, CH, C^3), 120.4 (dd, J=4.5, 58.5 Hz, CH, C^5), 128.2 (CH), 128.4 (CH), 128.5 (CH), 132.0 (t, J=5.4 Hz, CH, C^4), 135.8 (d, J=2.1 Hz, C), 140.2 (ddd, J=2.1, 43.5, 61.9 Hz, C^6), 149.2 (dt, J=2.6, 64.4 Hz, C^2), 168.9 (ddd, J=1.0, 2.1, 74.5 Hz, C^{1a}); MS (EI$^+$) m/z (%) 246 (M^++1, 0.1), 245 (M^+, 0.7), 91 (100); HRMS m/z 245.1239 ($^{13}C_4C_{11}H_{15}NO_2$ requires 245.1237).

4.5. Computational details

Since the mechanisms proposed here involve many open-shell singlet biradical species, we follow a well-established[17] technique, which requires geometry optimization at the DFT level of theory using an unrestricted broken-symmetry scheme (UBS)[18] followed by Brueckner doubles[19] [BD(T)] coupled-cluster single point computations. We decided to test the performance of the meta-GGA MPWB1K[20] functional, which has previously shown good performance in the determination of saddle-point geometries and activation energies, for modeling of reactions involving biradical intermediates. Thus, geometry optimizations were carried out using this functional and the 6-311+G** basis set. Harmonic frequencies were computed for all optimized species in order to characterize stationary points and to compute thermal contributions to free energies, which were computed at 34.7 atm (1 M standard state) and 423.15 K. Wavefunction stability check has been performed for species with potential biradical character.[21] Coupled-cluster BD(T) single point energy computations were performed using the frozen core approximation where core orbitals are excluded from cluster expansion and the cc-pVDZ[22] basis set in its spherical harmonics expression (5d). All computations were done with the Gaussian03 package.[23]

Acknowledgements

We thank CESGA for allocation of computer time and Xunta de Galicia INCITE08PXIB383129PR for financial support. J.-L.A.-G thanks Xunta de Galicia for a research contract under the Isidro Parga Pondal program. A.N.-V thanks Xunta de Galicia and Spanish Ministerio de Innovacion y Ciencia for research contracts under the Isidro Parga Pondal and Ramón y Cajal programs respectively.

Supplementary data

Cartesian coordinates for all computed structures; tables with absolute, ZPVE energies, imaginary frequencies and representation of associated vectors; ^{1}H and ^{13}C NMR spectra of **2**, **4**, and **5**. Supplementary data associated with this article can be found in online version, at doi:10.1016/j.tet.2010.03.035.

References and notes

1. Yonekura-Sakakibara, K.; Saito, K. *Nat. Prod. Rep.* **2009**, *26*, 1466–1487.
2. (a) Moyed, H. S.; Friedman, M. *Science* **1959**, *129*, 968–969; (b) Li, J.; Last, R. L. *Plant Physiol.* **1996**, *110*, 51–59.
3. Zhao, J.; Last, R. L. *Plant Cell* **1996**, *8*, 2235–2244.
4. von Nussbaum, F.; Spahl, W.; Steglich, W. *Phytochemistry* **1997**, *46*, 261–264.
5. (a) Miche, H.; Brumas, V.; Berthon, G. *J. Inorg. Biochem.* **1997**, *68*, 27–38; (b) Lee, J.; Chubb, A. J.; Moman, E.; McLoughlin, B. M.; Sharkey, C. T.; Kelly, J. G.; Nolan, K. B.; Devocelle, M.; Fitzgerald, D. J. *Org. Biomol. Chem.* **2005**, *3*, 3678–3685.
6. Kawai, M.; BaMaung, N. Y.; Fidanze, S. D.; Erickson, S. A.; Tedrow, J. S.; Sanders, W. J.; Vasudevan, A.; Park, C.; Hutchins, C.; Comess, K. M.; Kalvin, D.; Wang, J.; Zhang, Q.; Lou, P.; Tucker-Garcia, L.; Bouska, J.; Bell, R. L.; Lesniewski, R.; Henkin, J.; Sheppard, G. S. *Bioorg. Med. Chem. Lett.* **2006**, *16*, 3574–3577.
7. Thomas, G. J. *J. Agric. Food Chem.* **1984**, *32*, 747–749.
8. Verpoorte, R.; Choi, Y. H.; Kim, H. K. *Phytochem. Rev.* **2007**, *6*, 3–14.
9. Mustacich, D. J.; Bruno, R. S.; Traber, M. G. In *Vitamins and Hormones*; Litwack, G., Ed.; Elsevier: San Diego, CA, 2007; pp 1–21.
10. Alonso-Gomez, J. L.; Pazos, Y.; Navarro-Vazquez, A.; Lugtenburg, J.; Cid, M. M. *Org. Lett.* **2005**, *7*, 3773–3776.
11. Goldstein, E.; Beno, B.; Houk, K. N. *J. Am. Chem. Soc.* **1996**, *118*, 6036–6043.
12. Mottet, C.; Hamelin, O.; Garavel, G.; Deprés, J.-P.; Greene, A. E. *J. Org. Chem.* **1999**, *64*, 1380–1382.
13. Fleming, I.; Ramarao, C. *Org. Biomol. Chem.* **2004**, *2*, 1504–1510.
14. Boers, R. B.; Randulfe, Y. P.; van der Haas, H. N. S.; van Rossum-Baan, M.; Lugtenburg, J. *Eur. J. Org. Chem.* **2002**, 2094–2108.
15. To reduce computer costs and complexity of the potential surface we used vinyl ketenimine **3c**, allene aldehyde **8c**, and butynal **4c** as a model system, whose reaction energetics should not be essentially different to that of the experimental system.
16. Grimme, S. *Angew. Chem., Int. Ed.* **2006**, *45*, 4460–4464.
17. Schreiner, P. R.; Navarro-Vazquez, A.; Prall, M. *Acc. Chem. Res.* **2005**, *38*, 29–37.
18. (a) Cremer, D.; Filatov, M.; Polo, V.; Kraka, E.; Shaik, S. *Int. J. Mol. Sci.* **2002**, *3*, 604–638; (b) Polo, V.; Kraka, E.; Cremer, D. *Theor. Chem. Acc.* **2002**, *107*, 291–303.
19. Raghavachari, K.; Trucks, G. W.; Pople, J. A.; Head-Gordon, M. *Chem. Phys. Lett.* **1989**, *164*, 185–192.
20. Zhao, Y.; Truhlar, D. G. *J. Phys. Chem. A* **2004**, *108*, 6908–6918.
21. Bauernschmitt, R.; Ahlrichs, R. *J. Chem. Phys.* **1996**, *104*, 9047–9052.
22. (a) Dunning, T. H., Jr. *J. Chem. Phys.* **1989**, *90*, 1007–1023; (b) Davidson, E. R. *Chem. Phys. Lett.* **1996**, *260*, 514–518.
23. Frisch, M. J.; Trucks, G. W.; Schlegel, H. B.; Scuseria, G. E.; Robb, M. A.; Cheeseman, J. R.; Montgomery, J. A., Jr.; Vreven, T.; Kudin, K. N.; Burant, J. C.; Millam, J. M.; Iyengar,

S. S.; Tomasi, J.; Barone, V.; Mennucci, B.; Cossi, M.; Scalmani, G.; Rega, N.; Petersson, G. A.; Nakatsuji, H.; Hada, M.; Ehara, M.; Toyota, K.; Fukuda, R.; Hasegawa, J.; Ishida, M.; Nakajima, T.; Honda, Y.; Kitao, O.; Nakai, H.; Klene, M.; Li, X.; Knox, J. E.; Hratchian, H. P.; Cross, J. B.; Bakken, V.; Adamo, C.; Jaramillo, J.; Gomperts, R.; Stratmann, R. E.; Yazyev, O.; Austin, A. J.; Cammi, R.; Pomelli, C.; Ochterski, J. W.; Ayala, P. Y.; Morokuma, K.; Voth, G. A.; Salvador, P.; Dannenberg, J. J.; Zakrzewski, V. G.; Dapprich, S.; Daniels, A. D.; Strain, M. C.; Farkas, O.; Malick, D. K.; Rabuck, A. D.; Raghavachari, K.; Foresman, J. B.; Ortiz, J. V.; Cui, Q.; Baboul, A. G.; Clifford, S.; Cioslowski, J.; Stefanov, B. B.; Liu, G.; Liashenko, A.; Piskorz, P.; Komaromi, I.; Martin, R. L.; Fox, D. J.; Keith, T.; Al-Laham, M. A.; Peng, C. Y.; Nanayakkara, A.; Challacombe, M.; Gill, P. M. W.; Johnson, B.; Chen, W.; Wong, M. W.; Gonzalez, C.; Pople, J. A. *Gaussian 03, Revision E.01*; Gaussian: Wallingford, CT, 2004.